



Enhanced efficiency of polymer solar cells by improving molecular aggregation and broadening the absorption spectra



Weichao Chen^{a,d,*}, Wenfei Shen^{a,1}, Huan Wang^a, Fushuai Liu^b, Linrui Duan^b, Xiaofeng Xu^c, Dangqiang Zhu^{b,**}, Meng Qiu^b, Ergang Wang^{c,****}, Renqiang Yang^{b,***}

^a Collaborative Innovation Center for Eco-Textiles of Shandong Province, State Key Laboratory of Bio-Fibers and Eco-Textiles, College of Textiles & Clothing, Qingdao University, Qingdao, 266071, China

^b Qingdao Institute of Bioenergy and Bioprocess Technology, Chinese Academy of Sciences, Qingdao, 266101, China

^c Department of Chemical and Biological Engineering/Polymer Technology, Chalmers University of Technology, SE-412 96, Göteborg, Sweden

^d Key Laboratory of Science & Technology of Eco-Textile, Ministry of Education, Donghua University, Shanghai 200051, China

ARTICLE INFO

Keywords:

Polymer solar cells
Alkylthio-substituents
Molecular aggregation
Absorption spectra
High fill factor

ABSTRACT

Alkylthio-substituted thiophene-based benzo[1,2-*b*:4,5-*b'*]dithiophene (BDT) was used to construct PBDTS-DTBT, a medium band gap donor-acceptor (D-A) polymer with 5,6-difluoro-4,7-bis[4-(2-octyldodecyl)thiophene-2-yl]benzo[*c*] [1,2,5]thiadiazole (DTBT). The incorporation of sulfur atoms into the side chains not only lowered the highest occupied molecular orbital (HOMO) energy level but also improved molecular aggregation and thus afforded lower band gap (1.68 eV) with full width at half maximum (FWHM) of 170 nm in comparison to that of the analogous polymer (PBDT-DTBT) without sulfur atoms in side chains. Therefore, the bulk heterojunction polymer solar cells based on PBDTS-DTBT with 2% diiodooctane (DIO) as processing additive showed a high power conversion efficiency (PCE) of 9.73% with high open-circuit voltage (V_{OC} , 0.93 V), large short-circuit current density (J_{SC} , 14.23 mA/cm²) and high fill factor (FF, 0.735).

1. Introduction

Bulk heterojunction (BHJ) polymer solar cells (PSCs) have been extensively investigated because of their excellent properties such as flexibility, light weight and easy to fabricate. Therefore it possess potential applicability to fabricate large-area devices [1–6]. For single-junction PSCs, the power conversion efficiencies (PCE)s of such solar cells have been greatly improved and reached over 13% profiting from low band gap materials ($E_g < 1.6$ eV) and advanced device fabrication methods [3,7–10]. It is known that PCE is determined by the open-circuit voltage (V_{OC}), the short-circuit current density (J_{SC}) and fill factor (FF). In order to obtain high PCE, a lot of work has been done to broaden the absorption spectra or lower the highest occupied molecular orbital (HOMO) energy level of conjugated polymers in order to attain large J_{SC} and high V_{OC} , respectively. However, very often there is a trade-off between J_{SC} and V_{OC} , i.e., while V_{OC} is increased, J_{SC} is

reduced [11–13]. For example, the incorporation of F atoms in the backbone of a conjugated polymer could reduce the HOMO energy level resulting in high V_{OC} , but the absorption spectrum is blue-shifted with subsequent lowering of the J_{SC} [14–16]. Therefore, it is crucial to lower the HOMO energy level and widen the absorption spectra simultaneously to achieve high V_{OC} and large J_{SC} . In this regard, side chain engineering has been found to play a significant role in tuning the energy levels and absorption spectra of conjugated polymers [17–20]. It is notable that the polymers contain sulfur-based side chains, which usually showed unique photovoltaic characteristics owing to the fact that the sulfur atoms have both electron-donating and some π -acceptor capability [21–26].

Thus, alkylthio side chains have been paid much attention in recent years. In homogenous conjugated polymers, compared with alkyl side chains, the alkylthio side chains could expand the absorption spectra and lower the HOMO energy levels and as a result the polymers

* Corresponding authors. Collaborative Innovation Center for Eco-Textiles of Shandong Province, State Key Laboratory of Bio-Fibers and Eco-Textiles, College of Textiles & Clothing, Qingdao University, Qingdao, 266071, China.

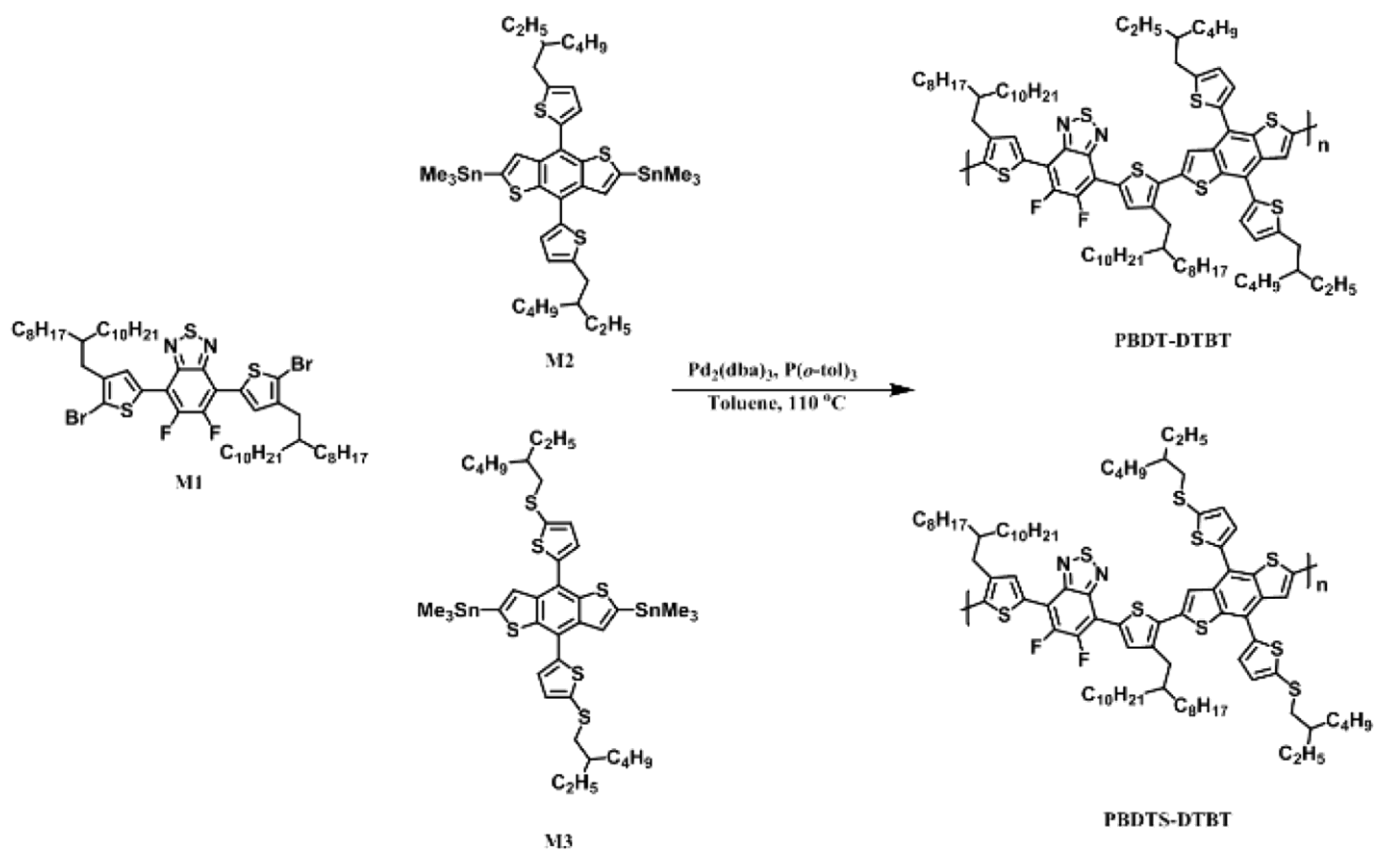
** Corresponding author.

*** Corresponding author.

**** Corresponding author.

E-mail addresses: chenwc@qdu.edu.cn (W. Chen), zhudq@qibebt.ac.cn (D. Zhu), ergang@chalmers.se (E. Wang), yangrq@qibebt.ac.cn (R. Yang).

¹ These authors contributed equally to this work.



Scheme 1. The synthetic routes towards PBDT-DTBT and PBDTS-DTBT.

exhibited high J_{SC} and V_{OC} values [17,27,28]. Recently, the effect of alkylthio side chain was further investigated in conjugated copolymers with electron-donating (D) and electron-accepting (A) units, which resulted in lowering the HOMO energy level [17,27–33]. Li and co-workers reported a low band-gap polymer named PBDTT-S-TT based on BDTT with branched alkylthio side chains, which showed high V_{OC} and good photovoltaic properties, due to a low-lying HOMO energy level [27]. The PCE was further improved by transforming the branched alkylthio side chains into linear alkylthio side chains. Wang and co-workers also used BDTT with alkylthio side chains to construct a high band-gap polymer named PBDTTS-FTAZ which demonstrated a high PCE of 8.3% owing to a high V_{OC} [28]. Notably, the polymers adorned with alkylthio side chains had lower HOMO energy levels but narrow red-shifted absorption spectra, compared with the analogous polymers containing alkyl side chains.

In this work, we designed and synthesized a medium band gap (1.68 eV) D-A polymer comprising of BDTT with alkylthio side chains and fluorinated benzothiadiazole (named PBDTS-DTBT, Scheme 1). The analogous polymer based on alkyl side chains (named PBDT-DTBT) was also synthesized for comparison. PBDTS-DTBT showed a lower HOMO energy level, stronger aggregation and thus a broader absorption spectrum than PBDT-DTBT. Therefore, the PSCs based on PBDTS-DTBT displayed a PCE of 9.73% with a V_{OC} of 0.93 V and a J_{SC} of 14.23 mA/cm². On the contrary the PBDT-DTBT-based devices exhibited a lower PCE of 7.00% with V_{OC} of 0.88 V and J_{SC} of 11.42 mA/cm². It is worth noting that the photovoltaic performance of PBDTS-DTBT is high in the literature for medium band gap donor polymers: PC₇₁BM system with alkylthio side chains [34,35].

2. Experimental

All raw materials and reagents were obtained from commercial sources and used directly without further purification. Toluene was

distilled over sodium/benzophenone and freshly distilled prior to use.

5,6-Difluoro-4,7-bis[4-(2-octyldodecyl)thiophene-2-yl] benzo[c][1,2,5]thiadiazole (M1) was purchased from Solarmer Materials (Beijing) Inc., (4,8-Bis(5-((2-ethylhexyl)thio)thiophen-2-yl)benzo[1,2-*b*:4,5-*b'*]dithiophene-2,6-diyl)bis(trimethylstannane) was synthesized according to the literature, ¹H NMR (600 MHz, CDCl₃), δ (ppm): 7.64 (t, 2H, $J = 15$ Hz), 7.34 (d, 2H, $J = 3.6$ Hz), 7.25 (d, 2H, $J = 3.6$ Hz), 2.94 (d, 4H, $J = 6.6$ Hz), 1.66 (m, 2H), 1.50 (m, 4H), 1.31 (m, 12H), 0.91 (m, 12H), 0.40 (m, 18H).

2.1. Synthesis of PBDTS-DTBT

Compounds M1 (211.1 mg, 0.2 mmol), M3 (193.8 mg, 0.2 mmol), Pd₂(dba)₃ (1.8 mg, 0.002 mmol), and P(*o*-tol)₃ (3.6 mg, 0.012 mmol) were added into a 25 mL flask. The flask was subjected to three successive cycles of vacuum followed by refilling with argon, and then dry toluene (5 mL) was added. The reaction mixture was heated to 110 °C for 2 h under argon protection. Then the mixture was cooled to indoor temperature, and the polymer was precipitated into methanol (100 mL), filtered, and purified by Soxhlet extraction with methanol, chloroform, and *o*-dichlorobenzene (*o*-DCB), respectively. The *o*-DCB solution was concentrated by evaporation and then precipitated into methanol. The black-blue solid was filtered to yield the desired polymer (141 mg, 65% yield). ¹H NMR (600 MHz, CDCl₃) δ 7.50–7.30 (br), 3.35–2.88 (br), 1.40–0.83 (br). Elemental analysis calcd (%) for C₈₈H₁₂₆F₂N₂S₉: C 68.64%, H 8.19%, S 18.72%; found: C 66.30%, H 9.55%, S 17.02%.

2.2. Fabrication and characterization of devices

Polymer solar cells were prepared with the device structure ITO/PEDOT: PSS/ Polymer: PC₇₁BM/PFN/Al. Patterned ITO-coated glasses were ultrasonically cleaned sequentially with ITO detergent, deionized water, acetone and isopropanol for 20 min each time, and then treated

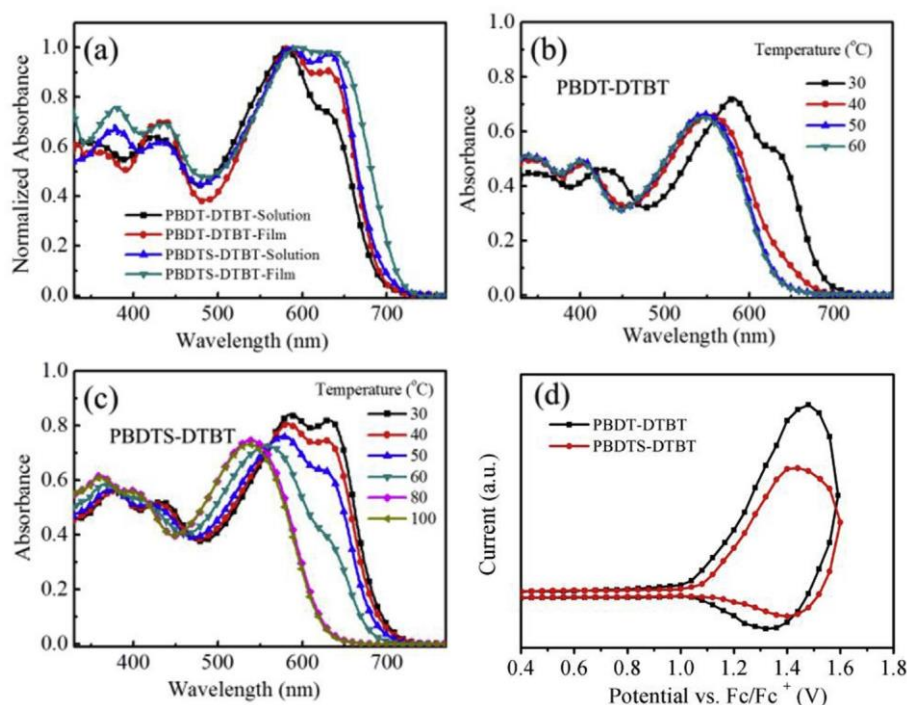


Fig. 1. (a) The normalized absorption spectra of PBDT-DTBT and PBDTS-DTBT in solution and as thin solid films, (b) The absorption spectra of PBDT-DTBT at different temperatures in 0.03 mg/mL solutions, (c) The absorption spectra of PBDTS-DTBT at different temperatures in 0.03 mg/mL solutions, (d) Cyclic voltammograms of as-casted films vs. the saturated calomel electrode (SCE) in 0.1 M $\text{Bu}_4\text{NPF}_6/\text{acetonitrile}$ solution, Fc/Fc^+ as internal reference.

with oxygen plasma for 6 min. ITO-coated glass substrates were covered with PEDOT: PSS (Baytron PVP Al 4083) upto about 35 nm thickness by spin coating, and then annealed at 160 °C for 30 min. Subsequently, the substrates were transferred to a glove box filled with N_2 . Different ratios of PBDT-DTBT/PBDTS-DTBT and PC_{71}BM (10 mg/mL, polymer) were dissolved in *o*-DCB and stirred overnight at room temperature because of the good solubility in *o*-DCB and CB. Likewise, the CB solutions (8 mg/mL, polymer) of different ratios of PBDT-DTBT/PBDTS-DTBT and PC_{71}BM were prepared and stirred overnight at room temperature. In a glove box, the solutions were spin-coated on PEDOT: PSS-modified ITO coated glass at 1250 rpm for 90s to prepare the active layers (*ca.* 100 nm) and then PFN solutions were spin-coated on top of the active layers at a speed of 2000 rpm. Finally, after the samples were transferred to a vacuum environment, Al (100 nm) were deposited at high vacuum via a mask to define the active area of 0.10 cm^2 . More than 10 devices were fabricated under the same condition [36].

The charge carrier mobilities of the two polymers were investigated by employing OFETs with bottom-gate/top-contact architecture. The polymers were deposited by spin-coating *o*-DCB solutions (5 mg/mL) on octadecyltrichlorosilane (OTS)-modified SiO_2/Si substrates at 3000 rpm. Cleaning of Si wafers and modification of OTS were performed according to reported procedures [37]._ENREF_36 Finally, gold source and drain contacts (30 nm thick) were deposited on the organic layer by vacuum evaporation through a shadow mask, affording OFETs with bottom-gate/top-contact configuration. The channel length (*L*) and width (*W*) were 31 and 273 μm , respectively. The mobilities were determined in the saturation region using the equation $\text{IDS} = (\mu\text{WC}_i/2L)(V_G - V_1)^2$, where C_i is the capacitance per unit area of the gate dielectric layer (10 nF/ cm^2). More than 5 devices were fabricated per polymer and tested in ambient conditions.

Thermogravimetric analysis (TGA) was conducted on a Perkin Elmer Pyris instrument under nitrogen atmosphere at a heating rate of 10 °C/min.

AFM measurements of film morphologies were imaged by an Agilent 5400 with tapping mode. TEM images were obtained on a Hitachi H-7650 transmission electron microscope at an accelerating voltage of 100 kV. A Hitachi U-4100 UV-vis-NIR scanning spectrophotometer was employed to measure absorption scope. A

concentration of about 0.02 mg/mL was used to measure the UV-vis spectra.

PCEs were obtained from current density-voltage (*J-V*) curves recorded by a Keithley 2420 source meter under illumination with an intensity of 100 mW/cm^2 (AM 1.5G). The light intensity was calibrated by a standard silicon photodiode. External quantum efficiencies (EQEs) of solar cells were analyzed by a certified Newport incident photon conversion efficiency (IPCE) measurement system.

3. Results and discussion

PBDT-DTBT and PBDTS-DTBT were synthesized by the Stille coupling reaction as depicted in Scheme 1. 2-Octyldodecyl side chains were incorporated on the thiophene moieties in DTBT to achieve good polymers solubility. Thus, both of the polymers could be dissolved excellently in common organic solvents such as chlorobenzene (CB) and *o*-dichlorobenzene (*o*-DCB). The molecular weights of the polymers were obtained by high temperature gel permeation chromatography (GPC) which using monodisperse polystyrene as the standard and 1,2,4-trichlorobenzene as the eluent at 150 °C. The number-average molecular weights (*M_n*) of PBDT-DTBT and PBDTS-DTBT were 22.7 kDa and 19.3 kDa separately with the corresponding polydispersity indices of 1.70 and 1.84.

Thermogravimetric analysis (TGA) (Fig. S1(a)) demonstrated that both PBDT-DTBT and PBDTS-DTBT exhibited good thermal stabilities for 375 °C and 433 °C respectively, with a weight-loss of 5% under N_2 atmosphere [38]. The higher decomposition temperature of PBDTS-DTBT indicated that the combination of sulfur atoms in the side chains could improve the thermal stability of the polymer [28].

The UV-vis absorption spectra of PBDT-DTBT and PBDTS-DTBT in *o*-DCB solutions and as thin films are shown in Fig. 1(a). In solution, PBDT-DTBT showed an evident absorption maximum at 582 nm and a shoulder at *ca.* 625 nm in long wavelength region. However, two marked absorption maxima were found at 585 and 635 nm in the spectrum of PBDTS-DTBT. Compared with PBDT-DTBT, PBDTS-DTBT showed a red-shifted absorption spectrum (*ca.* 10 nm). The observed difference in the absorption spectra of the two polymers could have been caused by molecular aggregation, and therefore, the temperature

Table 1
The optimal device parameters for PBDT-DTBT- and PBDTS-DTBT-based solar cells.

Devices	V_{oc} (V)	J_{sc} (mA/cm ²)	FF	PCE _{ave} (%) ^a	PCE _{max} (%)
PBDT-DTBT	0.88 (± 0.005)	11.26 (± 0.16)	0.688 (± 0.008)	6.86 (± 0.14)	7.00
PBDTS-DTBT	0.93 (± 0.005)	14.06 (± 0.17)	0.728 (± 0.007)	9.58 (± 0.15)	9.73

^a The average PCE was obtained from more than 10 devices.

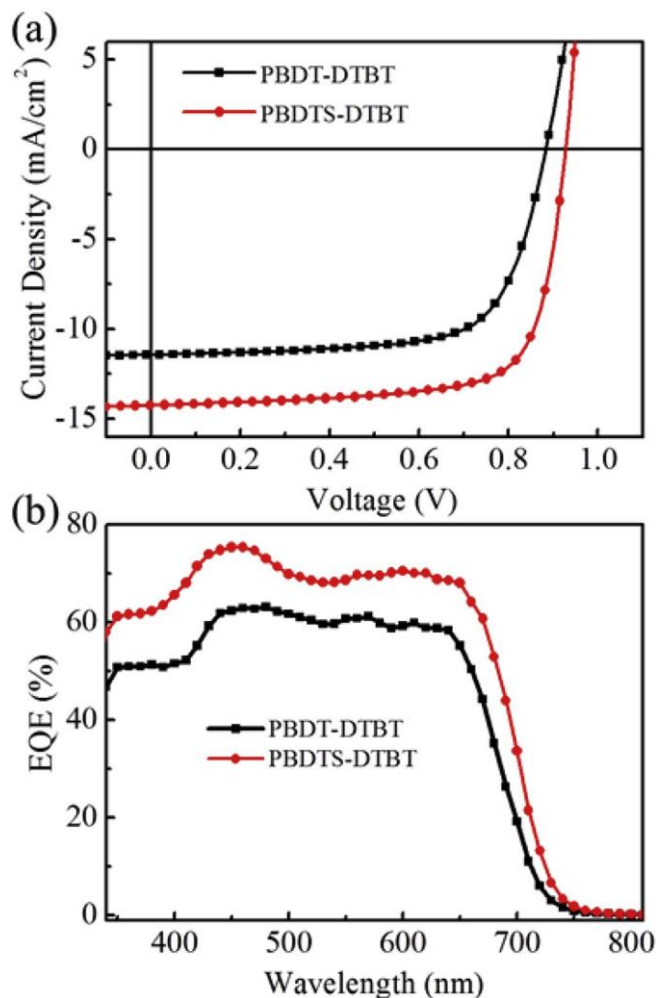


Fig. 2. (a) The J - V curves and (b) EQE spectra of optimal PBDTS-DTBT/PBDT-DTBT:PC₇₁BM polymer solar cells.

dependence of the absorption spectra was investigated and the results are in Fig. 1(b) and (c) for PBDT-DTBT and PBDTS-DTBT, respectively [3,39,40]. The absorption range of the polymers had different characteristics but both showed significant temperature dependence. In both cases, an obvious blue-shift was observed with the increasing of temperature. However, the absorption spectra of PBDTS-DTBT showed stronger temperature dependence compared with that of PBDT-DTBT. At elevated temperature, the absorption maximum at 635 nm in the spectrum of PBDTS-DTBT, which presumably originated from the strong intermolecular lamellar, which gradually became weak and finally completely disappeared at ca. 80 °C. The similar absorption maximum at 625 nm in the spectrum of PBDT-DTBT disappeared entirely at ca. 40 °C. In addition, with the temperature range from 30 °C to 80 °C, PBDTS-DTBT showed different absorption ability, but PBDT-DTBT almost showed same absorption ability with temperature higher than 40 °C. All of these evidences suggested that PBDTS-DTBT showed a stronger ability to aggregate in solution than PBDT-DTBT. Therefore, it is evident that the aggregation of PBDTS-DTBT could be enhanced

because of the incorporation of sulfur atoms on the side chains. In solid film, PBDTS-DTBT had a broader absorption than PBDT-DTBT as shown in Fig. 1(a). The main absorption region of PBDTS-DTBT is red-shifted by 20 nm with full width at half maximum (FWHM) of 170 nm in comparison to that of PBDT-DTBT (FWHM, 150 nm). It might have benefited from stronger aggregation of PBDTS-DTBT, which was attributed to the stronger electron-donating ability of the alkylthio group [27,41]. The optical band gaps were calculated to be 1.73 eV and 1.68 eV for PBDT-DTBT and PBDTS-DTBT, respectively, from the absorption onsets in the spectra of the thin solid films.

Cyclic voltammetry (CV) was employed to evaluate the frontier orbital energy levels of the polymers. The HOMO energy levels PBDT-DTBT and PBDTS-DTBT were calculated to be -5.46 eV and -5.54 eV, respectively, from the onsets of oxidation as shown in Fig. 1(d). Compared with PBDT-DTBT (see Fig. S1(b)), the HOMO level of PBDTS-DTBT was decreased by 0.08 eV approximately on account of the alkylthio side chains on BDTT moieties. This is consistent with the report by Cui et al. And higher V_{oc} could be expected from PBDTS-DTBT-based BHJ solar cells [27,41].

The LUMO energy levels PBDT-DTBT and PBDTS-DTBT were -3.73 eV and -3.86 eV according to the optical band gaps (1.73 eV vs. 1.68), respectively.

Organic field-effect transistors (OFETs) and vertical diodes were employed to analyse the effects of alkylthio side chains on the charge transport characteristics. Both of the polymers displayed p-channel characteristics and OFETs based on PBDTS-DTBT showed higher field-effect mobility (μ_{FET}) of $4.5 \times 10^{-2} \text{ cm}^2 \text{ V}^{-1} \text{ s}^{-1}$ than that of PBDT-DTBT ($8.5 \times 10^{-3} \text{ cm}^2 \text{ V}^{-1} \text{ s}^{-1}$). The typical output and transfer curves of the devices are shown in Fig. S2 (a, b) for PBDT-DTBT and Figs. S2(c and d) for PBDTS-DTBT. In the vertical direction, a vertical diode based on PBDTS-DTBT also showed higher mobility ($1.09 \times 10^{-4} \text{ cm}^2 \text{ V}^{-1} \text{ s}^{-1}$) than that of PBDT-DTBT ($7.49 \times 10^{-5} \text{ cm}^2 \text{ V}^{-1} \text{ s}^{-1}$) calculated using a space-charge-limited current model according to the current density-voltage (J - V) curves as shown in Fig. S3.

The effects of the alkylthio side chains on the photovoltaic properties were investigated with a conventional device structure of ITO/PEDOT: PSS/ Polymer: PC₇₁BM/PEN/Al. It was found that the devices based on PBDTS-DTBT: PC₇₁BM showed a PCE of 5.42% with high V_{oc} of 0.96 V, J_{sc} of 9.63 mA/cm² and FF of 0.586 in the optimal ratio (1:1.5, Fig. S4 (a)). When adding 2% DIO (Fig. S4 (b)) as processing additive, the PCE of 8.59% was achieved, with the J_{sc} and FF improved to 13.57 mA/cm² and 0.680, respectively. However, the PBDT-DTBT-based organic solar cells showed a very low PCE of 1.8%. When chlorobenzene was used to dissolve the polymers for further optimization, organic solar cells based on PBDT-DTBT: PC₇₁BM displayed high a PCE of 5.46% (Fig. S5 (a)). The performance was further improved to 7.00% upon addition of a little DIO (only 0.5%) (Fig. S5 (b)). For PBDTS-DTBT, the higher PCE of 9.73% was obtained through using CB and 2% DIO as solvent and additive, respectively. The optimal device parameters of the two polymers are listed in Table 1, and the typical current density-voltage (J - V) curves are displayed in Fig. 2(a). The PBDTS-DTBT-based devices showed higher PCE than PBDT-DTBT-based devices in both solvents, which benefitted from the higher V_{oc} , J_{sc} and FF.

The photoresponses of the optimized devices based on the two polymers were examined by measuring the external quantum

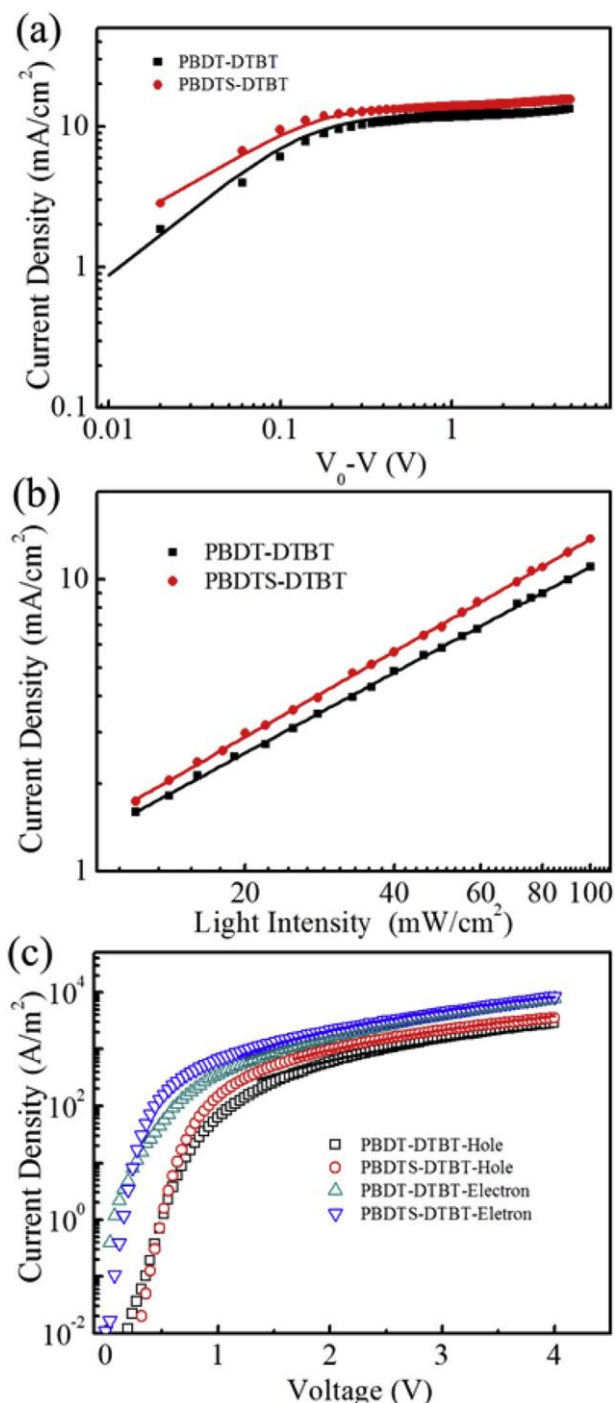


Fig. 3. (a) Photocurrent density (J_{ph}) versus effective voltage (V_{eff}) characteristics of the optimal devices. (b) Plots of current density versus the incident light intensity. (c) J - V curves of vertical diodes with the device structures of ITO/PEDOT:PSS/PBDT-DTBT:PC₇₁BM (1:2) or PBDTS-DTBT:PC₇₁BM(1:1.5)/Au for hole only devices, and ITO/ZnO/PBDT-DTBT:PC₇₁BM (1:2) or PBDTS-DTBT:PC₇₁BM (1:1.5)/PFN/Al for electron only devices. The solid lines are the fitting curves.

efficiencies (EQE)s. As shown in Fig. 2 (b), the PBDTS-DTBT-based devices showed broader photoresponses (350–730 nm) than the PBDT-DTBT-based devices (350–710 nm), which profited from the wider absorption spectra of PBDTS-DTBT (Fig. 1(a)). Moreover, higher EQE values with a peak over 70% were obtained in the -based devices, while the EQE values were only nearly 60% in the PBDT-DTBT-based devices. The current density obtained by integrating the EQE curve of the

PBDTS-DTBT devices with the standard AM 1.5G solar spectrum is about $13.89 \text{ mA}/\text{cm}^2$, which is slightly smaller than the measured value ($14.23 \text{ mA}/\text{cm}^2$) with an error of $< 5\%$. This means that the PBDTS-DTBT-based devices have stronger light absorption and therefore could harvest more photons and generate more excitons. These results prove that the introduction of alkylthio side chains could enhance light conversion efficiency and broaden the scope of absorption, thus obtained a higher J_{sc} , which was also proved by the saturation photocurrent density (J_{sat}). J_{sat} values were obtained by fitting the curves of photocurrent density (J_{ph}) versus effective voltage (V_{eff}). The curves of photocurrent density (J_{ph}) versus effective voltage (V_{eff}) are plotted in Fig. 3(a). Here, $J_{ph} = J_L - J_D$, where J_L and J_D stand for the current density under AM 1.5G illumination and in the dark, respectively, $V_{eff} = V_0 e V$, V_0 stands for the voltage at which $J_{ph} = 0$ and V is the applied voltage [20,32]. The figure clearly shows that the PBDTS-DTBT-based PSCs have a higher J_{sat} ($15.46 \text{ mA}/\text{cm}^2$) than PBDT-DTBT-based PSCs ($13.30 \text{ mA}/\text{cm}^2$), which illustrates that the PBDTS-DTBT-based PSCs have a higher maximum exciton generation rate (G_{max} , given by $J_{sat} = eG_{max}L$, where L is the thickness of the photoactive layer, which reflects the maximum photon absorption) than that of PBDT-DTBT-based PSCs. Under short-circuit condition, the higher ratio of J_{ph}/J_{sat} in PBDTS-DTBT:PC₇₁BM devices than in PBDT-DTBT:PC₇₁BM devices (92% vs. 86%) suggested that the photo-generated excitons were more efficiently when it separated into free holes and electrons and then they were collected free holes and electrons and then they were collected substantially at the electrodes with less recombination in the PBDTS-DTBT:PC₇₁BM devices. Therefore, sulfur atoms play a crucial role in broadening the absorption spectra and increasing J_{sc} . The power-law dependence of J_{sc} on the light intensity (I), i.e., J_{sc} vs. I^α , is shown in inset of Fig. 3(b). Consequently, PBDTS-DTBT-based devices have α value of 0.97 vs. 0.91 in PBDT-DTBT-based devices. An α value close to 1 revealed little bimolecular recombination in the PBDTS-DTBT-based devices [7,42].

The charge carrier transport characteristics in the blend films were investigated by employing space-charge-limited current model to measure the hole and electron mobilities [43]. As shown in Fig. 3 (c), the mobilities can be obtained by fitting the J - V curves of the diodes and the hole (μ_h) and electron (μ_e) mobilities for PBDTS-DTBT:PC₇₁BM and PBDT-DTBT:PC₇₁BM blend films are about $7.84 \times 10^{-5} \text{ cm}^2 \text{ V}^{-1} \text{ s}^{-1}$, $1.75 \times 10^{-4} \text{ cm}^2 \text{ V}^{-1} \text{ s}^{-1}$ and $4.94 \times 10^{-5} \text{ cm}^2 \text{ V}^{-1} \text{ s}^{-1}$, $1.42 \times 10^{-4} \text{ cm}^2 \text{ V}^{-1} \text{ s}^{-1}$ with a μ_e/μ_h ratio of 2.23 vs. 2.87, respectively. A relatively more balanced carrier transport was achieved in PBDTS-DTBT-based devices, which could be an important reason for the higher FF [8,44].

The morphologies of the blend films were characterized by atomic force microscopy (AFM) and transmission electron microscopy (TEM). As shown in Fig. 4 (a and b), the two polymers showed different surface morphologies, and the surfaces of the PBDT-DTBT films were relatively non-uniform with high root-mean-square (RMS) value of ca. 5.79 nm because of the large grains. However, the PBDTS-DTBT films showed relatively uniform surface with RMS value of ca. 4.12 nm. Thus, the PBDTS-DTBT:PC₇₁BM blend films had better interpenetrating network morphology than those of PBDT-DTBT:PC₇₁BM blend films as shown in Fig. 4(c and d). Therefore, the incorporation of sulfur atoms on the side chains could modify the surface morphology and bulk interpenetrating network, which might have been caused by the enhanced miscibility between polymers and PC₇₁BM.

4. Conclusions

A new medium band-gap conjugated polymer PBDTS-DTBT with alkylthio side chains was designed and synthesized. Compared with the analogous polymer PBDT-DTBT containing alkyl side chains, solar cell devices constructed from PBDTS-DTBT showed higher PCE of 9.73% with a higher V_{oc} of 0.93 V and an enhanced J_{sc} of $14.23 \text{ mA}/\text{cm}^2$. This was caused by the incorporation of sulfur atoms on the side chains, the

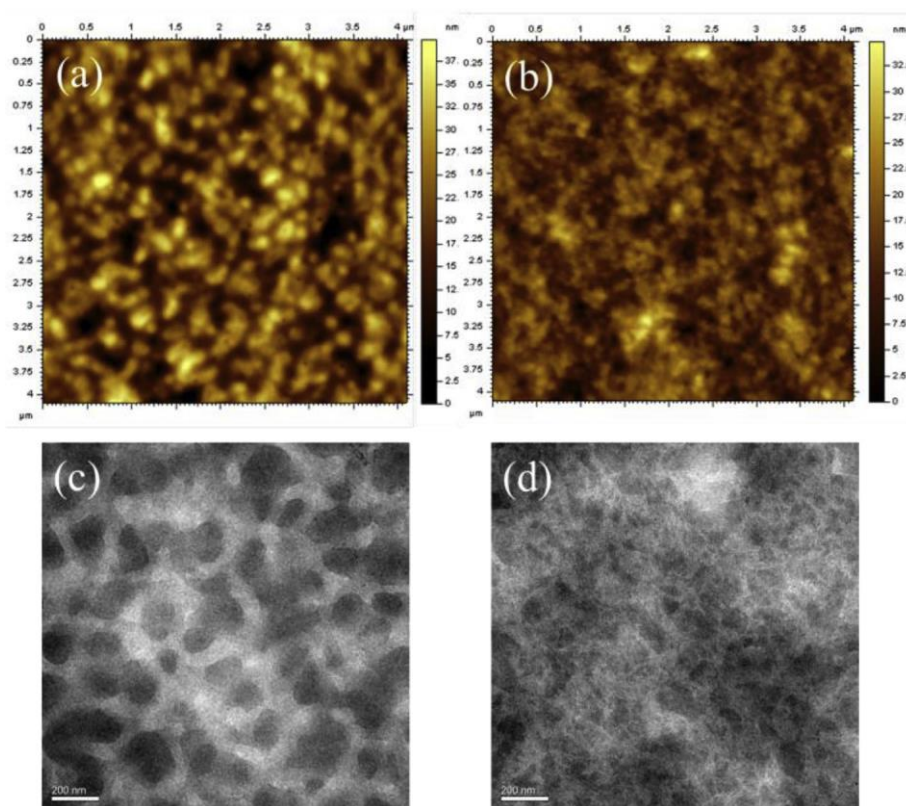


Fig. 4. (a) AFM and (c) TEM images of the PBDT-DTBT: PC₇₁BM blend films with 1:2 ratio, (b) AFM and (d) TEM images of the PBDTS-DTBT: PC₇₁BM blend films with 1:1.5 ratio.

which did not only lower the HOMO energy level but also broadened the absorption spectrum. In addition, good interpenetrating networks could be formed in the PBDTS-DTBT and PC₇₁BM blend films.

Acknowledgements

This work was supported by National Key R&D Program of China (2017YFB0309800), National Natural Science Foundation of China (21728401, 61405209, 51573205 and 21604092), Shandong Provincial Natural Science Foundation (ZR2016BB33).

Appendix A. Supplementary data

Supplementary data to this article can be found online at <https://doi.org/10.1016/j.dyepig.2019.03.014>.

References

- [1] Heeger AJ. 25th Anniversary Article. Bulk heterojunction solar cells: understanding the mechanism of operation. *Adv Mater* 2014;26:10.
- [2] Yao H, Ye L, Zhang H, Li S, Zhang S, Hou J. Molecular design of benzodithiophene-based organic photovoltaic materials. *Chem Rev* 2016;116:7397.
- [3] Liu Y, Zhao J, Li Z, Mu C, Ma W, Hu H, et al. Aggregation and morphology control enables multiple cases of high-efficiency polymer solar cells. *Nat Commun* 2014;5:5293.
- [4] Li Z, Jiang K, Yang G, Lai JYL, Ma T, Zhao J, et al. Donor polymer design enables efficient non-fullerene organic solar cells. *Nat Commun* 2016;7:13094.
- [5] He Z, Zhong C, Su S, Xu M, Wu H, Cao Y. Enhanced power-conversion efficiency in polymer solar cells using an inverted device structure. *Nat Photon* 2012;6:591.
- [6] Lin Y, Wang J, Zhang Z-G, Bai H, Li Y, Zhu D, et al. An electron acceptor challenging fullerenes for efficient polymer solar cells. *Adv Mater* 2015;27:1170.
- [7] Cui Y, Zhang S, Liang N, Kong J, Yang C, Yao H, et al. Toward efficient polymer solar cells processed by a solution-processed layer-by-layer approach. *Adv Mater* 2018;30:e1802499.
- [8] Nian L, Kan Y, Wang H, Gao K, Xu B, Rong Q, et al. Ternary non-fullerene polymer solar cells with 13.51% efficiency and a record-high fill factor of 78.13%. *Energy Environ Sci* 2018;11:3392–9.
- [9] Fan QP, Zhu QL, Xu Z, Su WY, Chen J, Wu JN, et al. Chlorine substituted 2D-conjugated polymer for high-performance polymer solar cells with 13.1% efficiency via toluene processing. *Nanomater Energy* 2018;48:413–20.
- [10] Li W, Ye L, Li S, Yao H, Ade H, Hou J. A high-efficiency organic solar cell enabled by the strong intramolecular electron push-pull effect of the nonfullerene acceptor. *Adv Mater* 2018;30:e1707170.
- [11] Zhang J, Zhang Y, Fang J, Lu K, Wang Z, Ma W, et al. Conjugated polymer–small molecule alloy leads to high efficient ternary organic solar cells. *J Am Chem Soc* 2015;137:8176.
- [12] Lu L, Zheng T, Wu Q, Schneider AM, Zhao D, Yu L. Recent advances in bulk heterojunction polymer solar cells. *Chem Rev* 2015;115:12666.
- [13] Chen W, Xiao M, Han L, Zhang J, Jiang H, Gu C, et al. Unsubstituted benzo-dithiophene-based conjugated polymers for high-performance organic field-effect transistors and organic solar cells. *ACS Appl Mater Interfaces* 2016;8:19665.
- [14] Jung JW, Liu F, Russell TP, Jo WH. Anthracene-based medium bandgap conjugated polymers for high performance polymer solar cells exceeding 8% PCE without additive and annealing process. *Adv Energy Mater* 2015;5:1500065.
- [15] Qiu M, Zhu D, Yan L, Wang N, Han L, Bao X, et al. Strategy to manipulate molecular orientation and charge mobility in D–A type conjugated polymer through rational fluorination for improvements of photovoltaic performances. *J Mater Chem C* 2016;120:22757.
- [16] Gu C, Zhu Q, Bao X, Wen S, Qiu M, Han L, et al. Dithieno[3,2-b:2',3'-d]silole-based low band gap polymers: the effect of fluorine and side chain substituents on photovoltaic performance. *Polym Chem* 2015;6:6219.
- [17] Cui C, He Z, Wu Y, Cheng X, Wu H, Li Y, et al. High-performance polymer solar cells based on a 2D-conjugated polymer with an alkylthio side-chain. *Energy Environ Sci* 2016;9:885.
- [18] Lee W, Lee C, Yu H, Kim D-J, Wang C, Woo HY, et al. Side chain optimization of naphthalenediimide–bithiophene-based polymers to enhance the electron mobility and the performance in all-polymer solar cells. *Adv Funct Mater* 2016;26:1543.
- [19] Wang T, Ravva MK, Brédas J-L. Impact of the nature of the side-chains on the polymer–fullerene packing in the mixed regions of bulk heterojunction solar cells. *Adv Funct Mater* 2016;26:5913.
- [20] Du Z, Chen W, Wen S, Qiao S, Liu Q, Ouyang D, et al. New benzo[1,2-b:4,5-b']dithiophene-based small molecules containing alkoxyphenyl side chains for high efficiency solution-processed organic solar cells. *Chem Sus Chem* 2014;7:3319.
- [21] Hou J, Fan B, Huo L, He C, Yang C, Li Y. Poly(alkylthio-p-phenylenevinylene): synthesis and electroluminescent and photovoltaic properties. *J Polym Sci A Polym Chem* 2006;44:1279.
- [22] Huo L, Zhou Y, Li Y. Alkylthio-substituted polythiophene: absorption and photovoltaic properties. *Macromol Rapid Commun* 2009;30:925.
- [23] Lee D, Stone SW, Ferraris JP. A novel dialkylthio benzo[1,2-b:4,5-b']dithiophene derivative for high open-circuit voltage in polymer solar cells. *Chem Commun* 2011;47:10987.

- [24] Lee D, Hubijar E, Kalaw GJD, Ferraris JP. Enhanced and tunable open-circuit voltage using dialkylthio benzo[1,2-b:4,5-b']dithiophene in polymer solar cells. *Chem Mater* 2012;24:2534.
- [25] Cui C, Wong WY. Effects of alkylthio and alkoxy side chains in polymer donor materials for organic solar cells. *Macromol Rapid Commun* 2016;37:287.
- [26] Min J, Cui C, Heumueller T, Fladischer S, Cheng X, Spiecker E, et al. Side-chain engineering for enhancing the properties of small molecule solar cells: a trade-off beyond efficiency. *Adv Energy Mater* 2016;6:1600515.
- [27] Cui C, Wong WY, Li Y. Improvement of open-circuit voltage and photovoltaic properties of 2D-conjugated polymers by alkylthio substitution. *Energy Environ Sci* 2014;7:2276.
- [28] Genene Z, Wang J, Meng X, Ma W, Xu X, Yang R, et al. High bandgap (1.9 eV) polymer with over 8% efficiency in bulk heterojunction solar cells. *Adv Electron Mater* 2016;2:1600084.
- [29] Li K, Li Z, Feng K, Xu X, Wang L, Peng Q. Development of large band-gap conjugated copolymers for efficient regular single and tandem organic solar cells. *J Am Chem Soc* 2013;135:13549.
- [30] Ye L, Zhang S, Zhao W, Yao H, Hou J. Highly efficient 2d-conjugated benzo-dithiophene-based photovoltaic polymer with linear alkylthio side chain. *Chem Mater* 2014;26:3603.
- [31] Kim J-H, Park JB, Jung IH, Yoon SC, Kwak J, Hwang D-H. New alkylthio-thieno [3,2-b]thiophene-substituted benzodithiophene-based highly efficient photovoltaic polymer. *J Mater Chem C* 2015;3:4250.
- [32] Kim J-H, Park JB, Yoon SC, Jung IH, Hwang D-H. Enhanced and controllable open-circuit voltage using 2D-conjugated benzodithiophene (BDT) homopolymers by alkylthio substitution. *J Mater Chem C* 2016;4:2170.
- [33] Wang K, Su W, Guo X, Zhang M, Li Y. Synthesis and photovoltaic properties of D-A copolymers based on alkylthio-thiophene or alkylthio-selenophene-BDT donor unit and DPP acceptor unit. *Org Electron* 2016;33:15.
- [34] Dong Y, Hu X, Duan C, Liu P, Liu S, Lan L, et al. A series of new medium-bandgap conjugated polymers based on naphtho[1,2-c:5,6-c]bis(2-octyl-[1,2,3]triazole) for high-performance polymer solar cells. *Adv Mater* 2013;25:3683.
- [35] Lan L, Zhang G, Dong Y, Ying L, Huang F, Cao Y. Novel medium band gap conjugated polymers based on naphtho[1,2-c:5,6-c]bis[1,2,3]triazole for polymer solar cells. *Polymer* 2015;67:40.
- [36] Shen W, Tang J, Wang Y, Liu J, Huang L, Chen W, et al. Strong enhancement of photoelectric conversion efficiency of Co-hybridized polymer solar cell by silver nanoplates and core-shell nanoparticles. *ACS Appl Mater Interfaces* 2017;9:5358.
- [37] Okamoto T, Jiang Y, Becerril HA, Hong S, Senatore ML, Tang ML, et al. Synthesis of regioregular pentacene-containing conjugated polymers. *J Mater Chem C* 2011;21:7078.
- [38] Hao L, Wang R, Fang K, Cai Y. The modification of cotton substrate using chitosan for improving its dyeability towards anionic microencapsulated nano-pigment particles. *Ind Crops Prod* 2017;95:348.
- [39] Zhou Y, Chen W, Du Z, Zhu D, Ouyang D, Han L, et al. High open-circuit voltage solution-processed organic solar cells based on a star-shaped small molecule end-capped with a new rhodanine derivative. *Sci China Chem* 2015;58:357.
- [40] Wang N, Chen W, Shen W, Duan L, Qiu M, Wang J, et al. Novel donor-acceptor polymers containing o-fluoro-p-alkoxyphenyl-substituted benzo[1,2-b:4,5-b]prime or minute]]dithiophene units for polymer solar cells with power conversion efficiency exceeding 9%. *J Mater Chem A* 2016;4:10212.
- [41] Gao Y, Saparbaev A, Zhang Y, Yang R, Guo F, Yang Y, et al. Efficient polymer solar cells based on poly(thieno[2,3-f]benzofuran-co-thienopyrroledione) with a high open circuit voltage exceeding 1 V. *Dyes Pigments* 2017;146:543.
- [42] Felekidis N, Wang E, Kemerink M. Open circuit voltage and efficiency in ternary organic photovoltaic blends. *Energy Environ Sci* 2016;9:257.
- [43] Zhu T, Zhang Y, Li Y, Song X, Liu Z, Wen S, et al. Acceptor-rich bulk heterojunction polymer solar cells with balanced charge mobilities. *Org Electron* 2017;51:16.
- [44] Gasparini N, Jiao X, Heumueller T, Baran D, Matt GJ, Fladischer S, et al. Designing ternary blend bulk heterojunction solar cells with reduced carrier recombination and a fill factor of 77%. *Nature Energy* 2016;1:16118.